DESIGN AND SIMULATION OF HENNA-BASED COMPOSITE SUBSTRATE FOR UHF-RFID APPLICATION ON DIELECTRIC PROPERTIES

Nadzeefah Zamil[1], M.N.M. Ansari[1], Y.E. Jalil[2], Noor Afeefah Nordin[1], Azlan, A.A.[3]
[1]Institute of Power Engineering, Universiti Tenaga Nasional, Selangor, Malaysia
[2]Department of Electrical and Electronics Engineering, Universiti Tenaga Nasional, Selangor, Malaysia.
[3]Politeknik Sultan Salahuddin Abdul Aziz Shah, Selangor, Malaysia
nadzeefah96, afeefahnordin1, 9m2agc (@gmail.com), ansari, yantierana (@uniten.edu.my)

ABSTRACT
This paper presented the effect of dielectric properties of henna-based composite towards the performance of the tag antenna for UHF-RFID application. The dielectric properties focused in this work were dielectric constant and loss tangent. Henna-based composite was developed with different amount of henna loading as the substrate for RFID passive tag. The design of antenna was optimized using CST Microwave software to achieve resonance frequency at 915 MHz. The output parameters from this work were reflection coefficient (dB), bandwidth (MHz), gain (dB), directivity (dBi), antenna efficiency (%) and voltage standing wave ratio (VSWR). In conclusion, dielectric properties of the substrate affect all the output parameters significantly except for directivity value.

Keywords: reflection coefficient, bandwidth, gain, directivity, VSWR

INTRODUCTION
Radio-Frequency Identification (RFID) gain its attention across the world since 1990's [1]. It is a system that can be used for item identifications, tracking activities and logistic purposes due to its flexibility, ready-ability and longer read range compared to barcode. RFID system is generally composed of three main components which are computer host, reader and tag. RFID tags can be divided into three categories based on type of their power supply which are active tag, semi-active tag and passive tag. As the reader send the electromagnetic wave to the passive tag, the antenna will inductively couple with IC chip, instruct the IC chip to reply its ID and the ID will be sent back to the reader via backscattering signal and finally, the data will be displayed in the computer host. The passive tag has become the most friendly-user because of its low cost, low maintenance and small in size since no battery is needed. Meanwhile, the performance of passive RFID tag depends on the properties of its antenna and substrate.

In RF application, the most popular commercial substrates are Rogers and FR-4. Rogers has a higher dielectric constant and remain stable although with higher frequencies and lower dissipation factor compared to FR-4. However, due to its expensive price, FR-4 is more affordable and commonly chosen for mass production. FR-4 is made from laminated epoxy with woven fiberglass sandwiched by copper sheet on both sides and has dielectric constant of 4.3. This rigid value of dielectric constant for FR-4 drives the researchers to look forward for flexibility by applying plant loading in the polymer during fabrication of substrate. The value of dielectric properties can be altered depending on the amount of plant loading since the plant contains higher weightage of carbon element.

The dielectric properties of the composite are depending on the polarization of the material [2] and amount of plant fiber loading [3]. This is due to interfacial and orientation polarization between filler (plant fiber) and matrix (polymers). As known, plant has permanent-polar molecule from the hydroxyl group which contributes to high hydrophilic characteristics while most of the polymers are non-polar [4]. Due to these circumstances, this will lead to interfacial and orientation polarization in the composite. The interfacial polarization occurred due to the difference of conductivity between two materials; the higher the differences of conductivity, the higher the interfacial polarization [5][6]. At the same time, orientation polarization occurred because of the existence of polar molecules in plant structure which is lignin, contributing to poor adhesion between filler and matrix [7]. *Table I* shows the example of composite with different type of plants.

Table I: Dielectric Constant Value (e') for different type of composites

Composites	Weightage (%)	Frequency Range (Hz)	Dielectric Constant Range (ε')
Jute/Bamboo/Polyester	15:15:70	3.0 – 6.0	3.50 – 5.50 [2]
Sisal/Polyester	50:50	0.7 – 4.2	3.25 – 3.55 [5]
Jute/Polypropylene	55.9:44.1	3.0 – 6.3	3. 10 – 7.10 [4]
Kenaf/Epoxy	14:86	12.4 G – 16.4 G	0.50 – 2.50 [6]

One of the methods to enhance adhesion between plant and polymer is chemical treatment such as sodium hydroxide (NaOH) or potassium permanganate ($KMnO_4$) [8][9]. The chemical treatment will help to remove the lignin structure from the plant and increase the roughness of the surface and will simultaneously reduce the hydrophilic nature of plant [10]. Reducing of OH^- in fibers will decrease the interfacial and orientation polarization occurred between fillers and composites. Thus, this work will discover the potential of henna-based composite for UHF-RFID application at 915 MHz with various value of dielectric constant and loss tangent.

METHODOLOGY
Preparation of Henna-Based Composite Substrate
Henna particles were oven-dried, sieved and treated with sodium hydroxide solution for 12 hours with a ratio of 1:20. The size of henna particles was kept constant not exceeding 150 μm. Then, the treated henna particles were dried in the oven for 24 hours after had been

washed by tap water for 3 times. Next, henna particles was mixed with epoxy polymer with different proportion before mixing with hardener for curing process. Finally, the mixture was poured in silicon mold for solidification process.

Dielectric Testing

The dielectric testing towards henna-based composite substrates was conducted using Agilent 85070 coaxial probe method based on ASTMB150 standard. They were placed between the fixtures which composed of a few holes and screwed up to tighten it. Then, the frequency was set between 860 – 960 MHz spesfically for ultra-high frequency. As the probe placed within the hole, the dielectric constant and loss tangent were measured and exported as raw data.

Simulation Work using CST Microwave Software

CST Microwave Software is the software to run the simulation especially for RF application to observe the behaviour of the antenna. The result of dielectric testing was implemented in CST Microwave software for simulation stage and the antenna design was optimized to maintain the resonance frequency at 915 MHz. ***Error! Reference source not found.*** and *Table II* show the design of the antenna using pure copper deposited on the henna-based composite. In order to determine the effect of dielectric properties towards the performance of tag is approaching accuracy, only m dimension was adjusted during optimization process and the resonance frequency was maintained at 915 ± 0.5 MHz (can refer *Table III*). This antenna design composed of capacitive loading, meandered line, T-matching loop, 18 Ω IC chip and a lumped element which is 0.8 pF capacitor. Each substrate is specified with an ID number based on dielectric constant value followed by loss tangent value. For example, the substrate that has 4.3 dielectric constant and 0.025 loss tangent is specified as 4325.

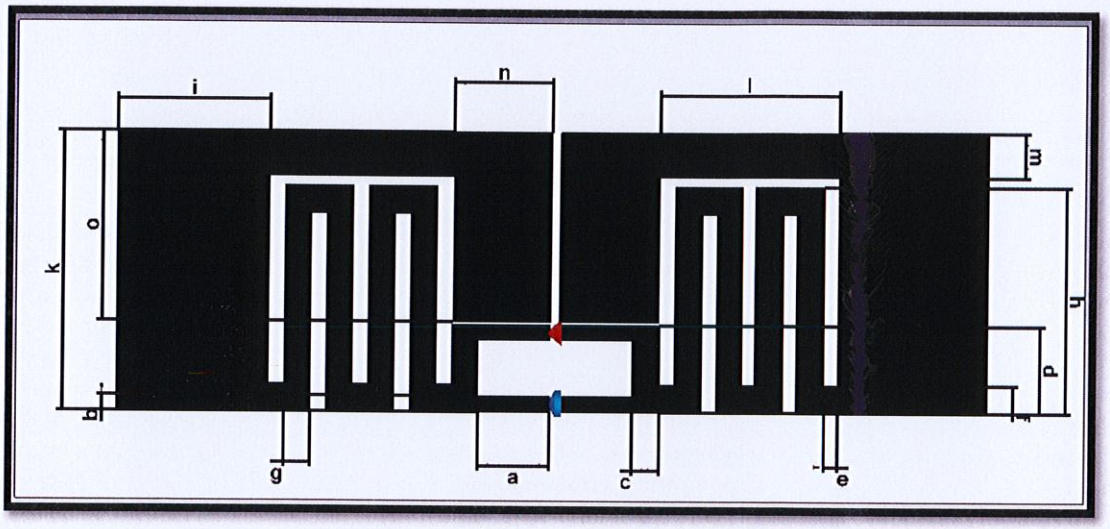

Figure 1. Design of antenna

Table II. Specification of antenna design

Name	Dimension (mm)
a	8.0
b	1.7
c	3.0
d	9.6
e	1.7
f	3.0
g	3.0
h	25.0
i	17.0
k	31.0
l	20.6
m	4.9
n	11.0
o	21.0

RESULTS AND DISCUSSION

In RFID application, the properties of the antenna really exert an impact towards the performance of tag. Nevertheless, the dielectric properties of the substrate also contribute to the tag performance although it is just a medium where the antenna, IC chip and lumped element are deposited. This is because the higher permittivity value of the substrate helps to reduce the dissipation of the RF wave. Hence, the main parameters of the dielectric properties that will be considered in this research are dielectric constant and loss tangent.

Effect on Reflection Coefficient and Bandwidth

In this context, the reflection coefficient or return loss describes the ratio of the complex amplitude of wave reflected from the tag antenna to the complex amplitude of wave transmitted from the reader where the reflection coefficient is considered accepted when it can go down below than -10 dB. Same goes to bandwidth, the bandwidth can be calculated by the difference between higher frequency and lower frequency where reflection coefficient is at -10 dB or VSWR is 2 which its value tells the amount of data can be transmitted. *Figure 2* shows result of reflection coefficient with various value of dielectric constant and loss tangent. As the value of dielectric constant increases, the value of reflection coefficient decreases which is good for performance of the tag. Higher dielectric constant and lower loss tangent values will shift the resonance frequency to the left. Hence, the m dimension needs to be increased so that the resonance frequency at 915 MHz can be achieved. Lowest reflection coefficient was experienced by 4335 and followed by 3825. Meanwhile, the calculation of the bandwidth had been calculated and tabulated in *Table III*. By comparing various value loss tangent, it shows that bigger bandwidth could be obtained by applying higher loss tangent. This can be observed by comparing 4345 with 4325 and 4335.

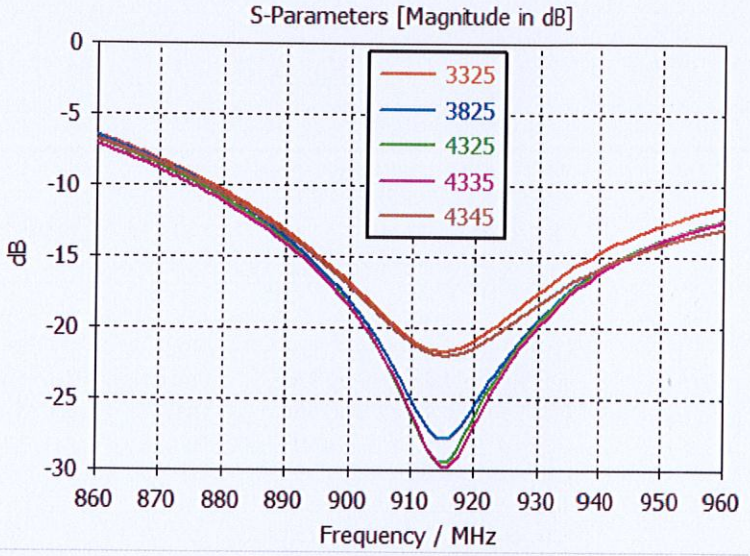

Figure 2. Result of reflection coefficient

Effect on Gain, Directivity and Antenna Efficiency

Antenna directivity describes the degree of the RF wave transmitted where antenna gain refers to the intensity of the RF wave in particular degree. The product of directivity and antenna efficiency can be expressed as the value of gain. In other word, the value of gain depends on the value of directivity and antenna efficiency. *Figure 3 and Figure 4* show the radiation pattern of gain and directivity for each substrate respectively with omnidirectional pattern since it is dipole antenna. Based on *Table III*, it is clear that higher gain can be obtained by applying lower loss tangent substrate. The directivity value keeps increases as the value of dielectric constant and loss tangent also increase but not very significantly. This is proven that dipole antenna has omnidirectional properties of radiation compared to directive antenna such as Yagi. However, the highest gain and antenna efficiency was achieved by 3825 and followed by 3325.

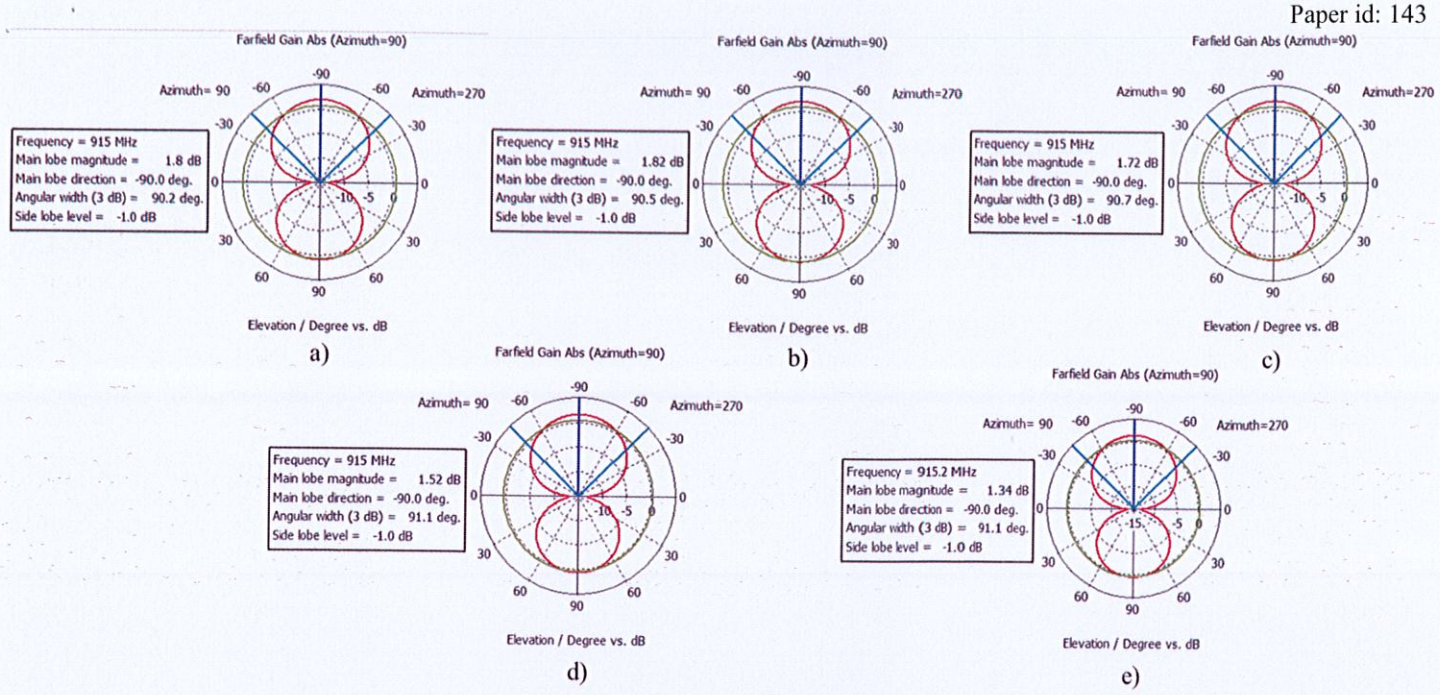

Figure 3. Various value of gain where a) 3325, b) 3825, c) 4325, d) 4335 and e) 4345

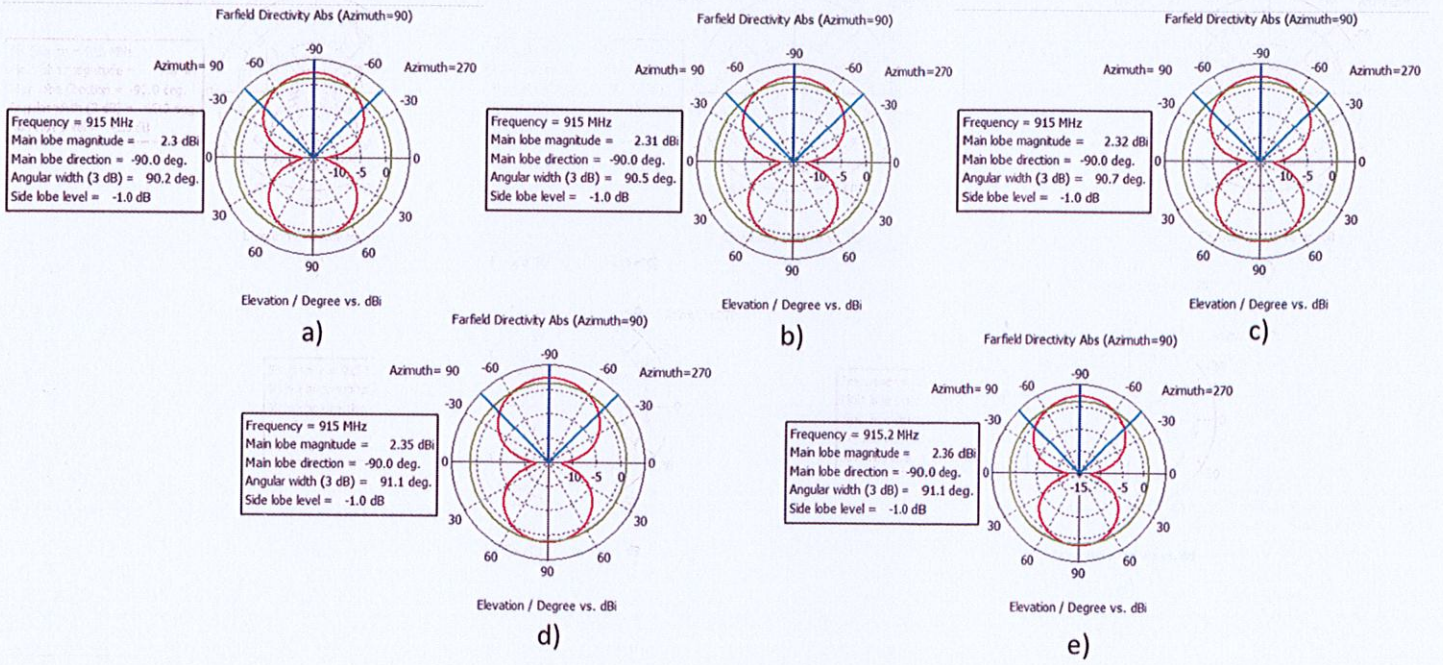

Figure 4. Various value of directivity where a) 3325, b) 3825, c) 4325, d) 4335 and e) 4345

Effect on VSWR

VSWR stands for Voltage Standing Wave Ratio describes the efficiency of the power received from the reader to the antenna. As the power received decreases, the antenna might have not enough power to transmit back. The ideal value of VSWR with 0% reflected power is 1:1. Hence, the best VSWR that can be achieved in this research is 1.07 experienced by 4325 and 4335. **Error! Reference source not found.** showed the summarization of simulation result.

Table III. Summarization of simulation result

ID Number	Dielectric Constant	Loss Tangent	m (mm)	Resonance Frequency (MHz)	Reflection Coefficient (dB)	Bandwidth (MHz)	Gain (dB)	Directivity (dBi)	Antenna Efficiency (%)	VSWR
3325	3.3	0.025	1.80	915.0	-21.63	102.27	1.80	2.30	78.26	1.18
3825	3.8	0.025	2.95	915.0	-27.79	203.44	**1.82**	2.31	**78.79**	1.09
4325	4.3	0.025	4.90	915.0	-29.46	175.97	1.72	2.32	74.14	**1.07**
4335	4.3	0.035	3.50	915.1	**-29.68**	195.75	1.52	2.35	64.68	**1.07**
4345	4.3	0.045	2.67	915.1	-22.02	**205.09**	1.33	**2.36**	56.36	1.17

Effect of Substrate Thickness Towards the Tag Performance

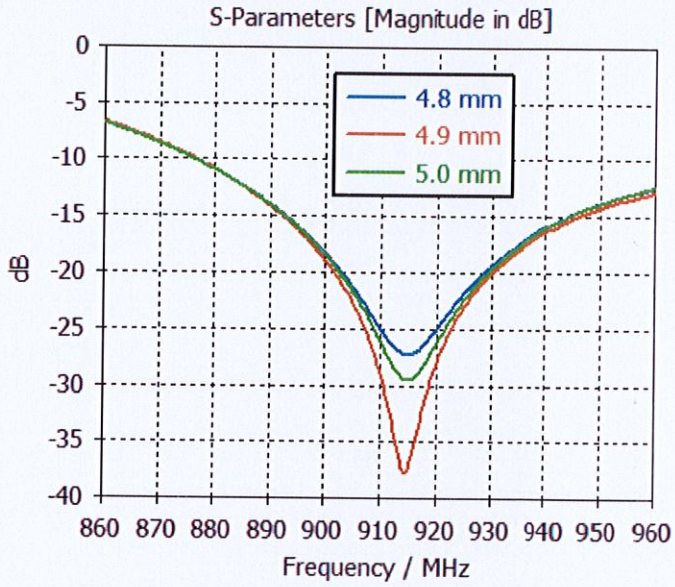

m (mm)	Substrate Thickness (mm)	Resonance Frequency (MHz)	Reflection Coefficient (dB)	Bandwidth (MHz)	Gain (dB)	Directivity (dBi)	Antenna Efficiency (%)	VSWR
4.90	5.0	915.0	-29.46	175.97	1.72	**2.32**	0.74	1.07
3.95	4.9	914.5	**-37.69**	193	**1.824**	**2.32**	**0.79**	**1.03**
3.30	4.8	915.0	-27.21	**200.86**	1.818	**2.32**	0.78	1.09

CONCLUSION

The amount of henna loading can give different value of dielectric properties which contributes to flexibility of substrate in UHF-RFID application. Based on these simulation result, (1) lowest reflection coefficient experienced by 4334, (2) bigger size of bandwidth can be achieved by implementing higher loss tangent, (3) highest gain and antenna efficiency was achieved by 3825 (4) directivity has changed but not so significant due to properties of dipole antenna which radiated omnidirectional wave and (5) the best VSWR was obtained by

4325 and 4335. In conclusion, higher dielectric constant contributes to stability of overall performance as the value of reflection coefficient significantly decreased.

ACKNOWLEDGEMENT

The authors would like to thank Innovative Research and Management Centre (iRMC), Universiti Tenaga Nasional for BOLD grant project number RJO10517844-105 for the funding, Department of Mechanical and Electrical Engineering, Universiti Tenaga Nasional and Antenna Research Centre, UiTM Shah Alam for providing the facilities to complete this research.

REFERENCES

[1] C. C. Lee, S. Der Chen, C. T. Li, C. L. Cheng, and Y. M. Lai, "Security enhancement on an RFID ownership transfer protocol based on cloud," *Futur. Gener. Comput. Syst.*, vol. 93, pp. 266–277, 2019, doi: 10.1016/j.future.2018.10.040.

[2] E. Jayamani, S. Hamdan, M. R. Rahman, and M. K. Bin Bakri, "Comparative study of dielectric properties of hybrid natural fiber composites," *Procedia Eng.*, vol. 97, no. December, pp. 536–544, 2014, doi: 10.1016/j.proeng.2014.12.280.

[3] M. A. A. Mohsin, L. Iannucci, and E. S. Greenhalgh, "Fibre-volume-fraction measurement of carbon fibre reinforced thermoplastic composites using thermogravimetric analysis," *Heliyon*, vol. 5, no. 1, p. e01132, 2019, doi: 10.1016/j.heliyon.2019.e01132.

[4] G. George, K. Joseph, E. R. Nagarajan, E. Tomlal Jose, and K. C. George, "Dielectric behaviour of PP/jute yarn commingled composites: Effect of fibre content, chemical treatments, temperature and moisture," *Compos. Part A Appl. Sci. Manuf.*, vol. 47, no. 1, pp. 12–21, 2013, doi: 10.1016/j.compositesa.2012.11.009.

[5] P. A. Sreekumar, J. M. Saiter, K. Joseph, G. Unnikrishnan, and S. Thomas, "Electrical properties of short sisal fiber reinforced polyester composites fabricated by resin transfer molding," *Compos. Part A Appl. Sci. Manuf.*, vol. 43, no. 3, pp. 507–511, 2012, doi: 10.1016/j.compositesa.2011.11.018.

[6] M. J. M. Ridzuan, L. S. S. Liew, M. S. A. Majid, E. M. Cheng, A. Khasri, and A. Z. A. Firdaus, "Dielectric properties of kenaf filled epoxy composites," *IOP Conf. Ser. Mater. Sci. Eng.*, vol. 670, no. 1, 2019, doi: 10.1088/1757-899X/670/1/012047.

[7] A. Saidah, Y. Yudinata, and S. E. Susilowati, "Design of composite material of rice straw fiber reinforced epoxy for automotive bumper," *3rd Int. Conf. Comput. Eng. Des. ICCED 2017*, vol. 2018-March, pp. 1–4, 2018, doi: 10.1109/CED.2017.8308105.

[8] J. E. R. Dhas, P. Pradeep, D. Gladson, R. Dinesh, and M. Aran, "Comparison of mechanical properties for alkali treated and untreated palm/glass sandwiched fiber reinforced polymer composite," *Proc. Int. Conf. Recent Adv. Aerosp. Eng. ICRAAE 2017*, pp. 1–5, 2017, doi: 10.1109/ICRAAE.2017.8297216.

[9] Z. Xia, J. Y. Xu, and X. G. Li, "Effect of alkaline treatment of straw fiber on mechanical properties of cement-bonded straw fiber board," *2010 Int. Conf. Mech. Autom. Control Eng. MACE2010*, no. 2008, pp. 3006–3008, 2010, doi: 10.1109/MACE.2010.5536208.

[10] M. A. Kassim, M. N. A. M. Taib, M. A. Jamaludin, N. Zakaria, and K. Nordin, "Mechanical properties of treated Kenaf (Hibiscus cannabinus) polyester composite at different alkaline concentration," *BEIAC 2013 - 2013 IEEE Bus. Eng. Ind. Appl. Colloq.*, pp. 421–424, 2013, doi: 10.1109/BEIAC.2013.6560161.

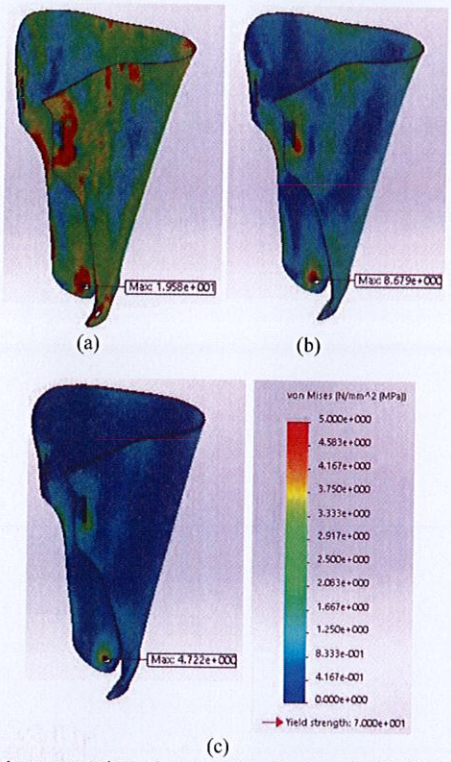

Fig. 7: Resultant von Misses Stress of the shank part with thickness of (a) 0.5 mm, (b) 1.0 mm, and (c) 1.5 mm

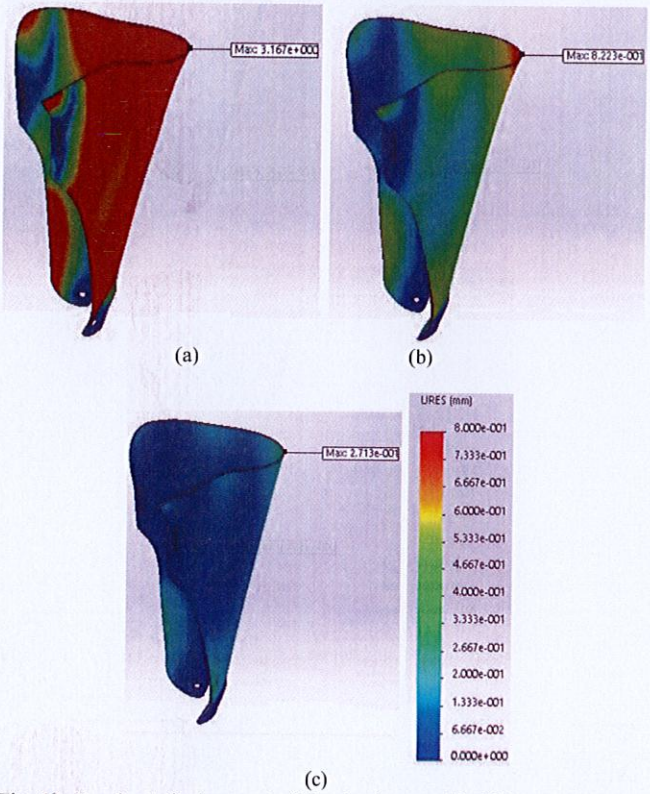

Fig. 12: Resultant displacement of the shank part with thickness 0.5 mm, 1.0 mm, and 1.5 mm

3.3. Fabrication of Adjustable Ankle Foot Orthosis

3D Printer is used to construct the ankle foot orthosis. In this project, PLA is chosen as the material because it is a well-known and widely used biodegradable polymer. Researchers also agreed that PLA is an ideal material to be used in biomedical field, as it is biocompatible with environmental concerns [12].

Ankle joints are purchased to assemble the two braces. The joints are made from rubber and are specially intended to be used for prosthetics. Straps, belts, and shoe insole are also purchased as finishing to the product as shown in Fig. 13.

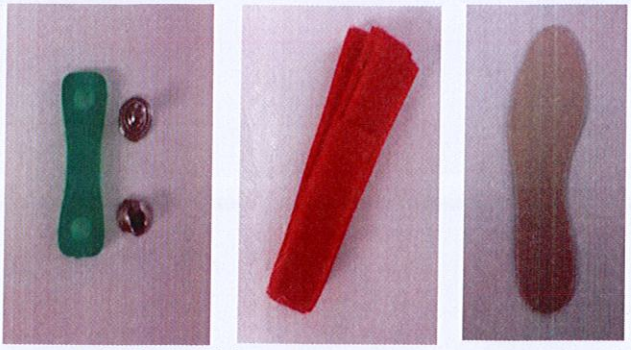

Fig. 13: Ankle joints, adhesive straps and shoe insole

The foot part and shank part are extruded separately. For the shank part, the height of the entire model is 310 mm while the maximum model height that can be constructed using the 3D printer is only 200 mm. therefore, the shank part is split into two parts in order to fit the model into the 3D printer. The extruded parts and purchased parts are then assembled together in the final product as shown in Fig. 14.

This project is believed to be a significant potential to help cerebral palsy children because this condition is considered chronic and the cure is not yet discovered. The effects of having equinus foot, especially abnormal walking gait can persist through lifetime if left untreated. Efficient and effective walking is an important treatment goal for children with cerebral palsy because mobility is associated with functional independence and participation of the child in society. Therefore, physical therapy is an essential component in the treatment of these children.

Fig. 8: Side view and front view of final product

4. Conclusion

This project is revolving around three main objectives, which are designing an adjustable ankle foot orthosis for cerebral palsy children, performing computational analysis on the design, and also constructing the model using 3D printing technology. The design is made by proper conceptual evaluation. Based on the three initial ideas, one is selected by using Pugh Method. Then, analysis is performed on the conceptual design. The model with thickness of 1.5 mm produces the best result, as compared to thinner model. The maximum value of von misses Stress under this condition for

foot part is 45.7 MPa, while the maximum displacement is 3.9 mm. Meanwhile for the shank part, the maximum resultant values of Von Misses Stress and displacement are 4.7 MPa and 0.3 mm respectively. These values indicate that the design is feasible. Lastly, the model is fabricated using 3D printing technology. Specific procedures and settings are conducted to achieve the best outcome.

Acknowledgment

This research was supported by Universiti Teknologi MARA, UiTM under Grant No. 600-IRMI/DANA 5/3/BESTARI(P) (103/2018). We thank and acknowledge our colleagues from Faculty of Medicine, Universiti Teknologi MARA who provided insight and expertise that greatly assisted the research.

References

[1] R. E. Schneider *et al.*, "The Association between Maternal Age and Cerebral Palsy Risk Factors," *Pediatr. Neurol.*, 2018.

[2] X. Liu *et al.*, "Long-Term Effects of Orthoses Use on the Changes of Foot and Ankle Joint Motions of Children With Spastic Cerebral Palsy," *PM&R*, pp. 1–7, 2017.

[3] A. Szopa, "Clinical Biomechanics Postural orientation and standing postural alignment in ambulant children with bilateral cerebral palsy," vol. 49, no. August, pp. 22–27, 2017.

[4] M. Kadhim and F. Miller, "Gait & Posture Crouch gait changes after planovalgus foot deformity correction in ambulatory children with cerebral palsy," *Gait Posture*, vol. 39, no. 2, pp. 793–798, 2014.

[5] S. A. Galey, Z. F. Lerner, T. C. Bulea, S. Zimbler, and D. L. Damiano, "Effectiveness of surgical and non-surgical management of crouch gait in cerebral palsy: A systematic review," *Gait Posture*, vol. 54, pp. 93–105, 2017.

[6] J. Machida, Y. Inaba, and N. Nakamura, "Management of foot deformity in children," *J. Orthop. Sci.*, vol. 22, no. 2, pp. 175–183, 2017.

[7] S. Eqtiinus, "Pediatric Spastic Equinus Deformity."

[8] A. Agarwal and I. Verma, "Review article Cerebral palsy in children : An overview," *J. Clin. Orthop. Trauma*, vol. 3, no. 2, pp. 77–81, 2012.

[9] T. J. Hagedorn, I. R. Grosse, and S. Krishnamurty, "A concept ideation framework for medical device design," *J. Biomed. Inform.*, vol. 55, pp. 218–230, 2015.

[10] J. Karl, J. Torres, and A. L. I. P. Gordon, "Mechanical Property Optimization of FDM PLA in Shear with Multiple Objectives," vol. 67, no. 5, pp. 1183–1193, 2015.

[11] V. K. Nandikolla, R. Bochen, S. Meza, and A. Garcia, "Experimental Gait Analysis to Study Stress Distribution of the Human Foot," vol. 2017, 2017.

[12] G. Glenn, A. Klamczynski, and Z. S. Petrovi, "Biodegradability study of polylactic acid / thermoplastic polyurethane blends Vladislav Ja," vol. 47, pp. 7–9, 2015.